Computing Bisimulation Functions using SOS Optimization and δ-Decidability over the Reals

Abhishek Murthy
Stony Brook University
Stony Brook, NY, USA
amurthy@cs.sunysb.edu

Md. Ariful Islam
Stony Brook University
Stony Brook, NY, USA
mdaislam@cs.sunysb.edu

Scott A. Smolka
Stony Brook University
Stony Brook, NY, USA
sas@cs.sunysb.edu

Radu Grosu
Vienna Univ. of Technology
Vienna, Austria
radu.grosu@tuwien.ac.at

ABSTRACT

We present BFComp, an automated framework based on Sum-Of-Squares (SOS) optimization and δ-decidability over the reals to compute Bisimulation Functions (BFs) that characterize input-to-output stability of dynamical systems. BFs are Lyapunov-like functions that decay along the trajectories of a given pair of systems, and can be used to establish the stability of the outputs with respect to bounded input deviations.

In addition to establishing IOS, BFComp is designed to provide tight bounds on the squared output errors between systems whenever possible. For this purpose, two SOS optimization formulations are employed: SOSP 1, which enforces the decay requirements on a discretized grid over the input space, and SOSP 2, which covers the input space exhaustively. SOSP 2 is attempted first, and if the resulting error bounds are not satisfactory, SOSP 1 is used to compute a *Candidate BF* (CBF). The decay requirement for the BFs is then encoded as a δ-decidable formula and validated over a level set of the CBF using the dReal tool. If dReal produces a counterexample comprising the states and inputs where the decay requirement is violated, this pair of vectors is used to refine the input-space grid and SOSP 1 is iterated.

By computing BFs that appeal to a small-gain theorem, the BFComp framework can be used to show that a subsystem of a feedback-composed system can be replaced–with bounded error–by an approximately equivalent abstraction, thereby enabling approximate model-order reduction of dynamical systems. We illustrate the utility of BFComp on a canonical cardiac-cell model, showing that that the four-variable Markovian model for the slowly activating Potassium current I_{Ks} can be safely replaced by a one-variable Hodgkin-Huxley-type approximation.

1. INTRODUCTION

Input-to-State Stability (ISS) of a pair of dynamical systems refers to the property that bounded differences in their input signals lead to bounded differences in their resulting state trajectories. *Input-to-Output Stability* (IOS) generalizes ISS to systems with output maps. Since the seminal work of Sontag [27, 28, 29], the $\mathcal{K}$, $\mathcal{KL}$, and $\mathcal{K}_\infty$ classes of Kamke functions have been used to characterize ISS of dynamical systems as extensions of Lyapunov stability; see [16]. These Lyapunov-like functions have been used in the small-gain theorems of [32] to establish stability of feedback-based interconnected systems, thereby enabling compositional design of nonlinear control systems.

Similar to Kamke and Lyapunov functions, *Bisimulation Functions* (BFs) have played a transformative role in extending the control-theoretic notions of Lyapunov Stability and ISS to system verification. BFs [7, 8, 9, 1, 13] are Lyapunov-like functions that decay along the trajectories of a given pair of dynamical systems. Level sets of BFs yield approximate bisimulation relations that generalize the classical notion of bisimulation equivalence of finite-state systems [21] to real-valued continuous-time dynamical systems. BFs also allow one to show that a system is robust to bounded deviations in the input signals.

BFs can also be used to reason *compositionally* about dynamical systems. Consider a dynamical system D with a subsystem S connected to the rest of D through a feedback loop. Moreover, suppose we have an approximately equivalent version S' of S that uses fewer state variables than S. That is, S' is an *abstraction* or model-order reduction of S, and by substituting S' for S in D one would hope to obtain the corresponding model-order reduction in D. Care must be taken in this situation, however, as the approximation error between S and S' may get amplified by the feedback context in which S resides.

As shown in [1, 19], one can appeal to a small-gain theorem to compute BFs that *bound the error* that is introduced when substituting S' for S within D. BFs can also be used in other system design and verification settings, including controller design [10], reachability analysis [17], and simulation-based verification [11, 3].

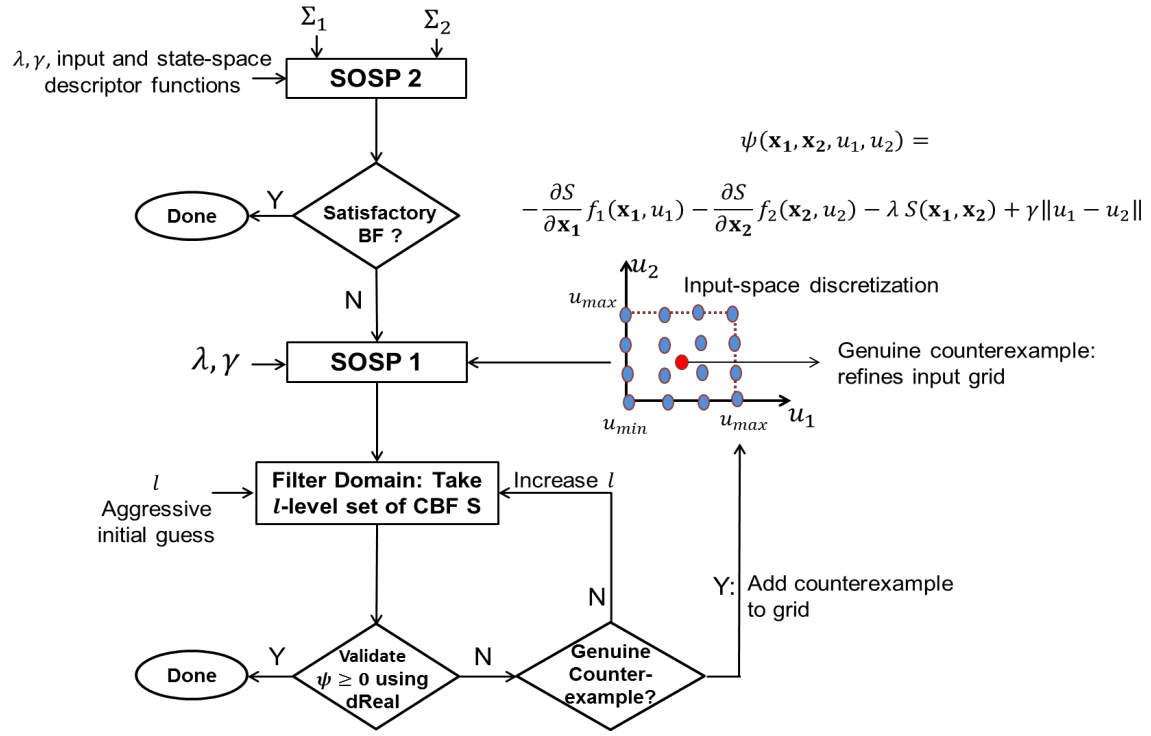

Figure 1: BFComp: An Automated Framework for Computing BFs using SOS Optimization and δ-decidability.

In this paper, we present BFComp: *an automated framework for computing BFs that characterize IOS of dynamical systems*. BFComp, which is illustrated in Fig. 1, leverages Sum-Of-Squares (SOS) optimization and δ-decidability over the reals [6], a new form of Satisfiability Modulo Theory (SMT), to compute BFs. In addition to establishing IOS, BFComp is designed to provide tight bounds on the squared output errors between systems whenever possible.

An overview of BFComp is as follows. Given a pair of dynamical systems Σ_1 and Σ_2, an SOS Problem (SOSP) called SOSP 2 is formulated and solved using MATLAB SOSTOOLS [24]. SOSP 2 requires the decay parameter λ, the gain parameter γ, and so-called *descriptor functions* that characterize the bounded state and input spaces. If the resulting BF provides satisfactory bounds on the output error, then the BF computation terminates.

Otherwise, an alternative SOSP formulation, SOSP 1, is called upon. SOSP 1, which we recently proposed in [19], uses λ and γ to compute a *Candidate BF* (CBF) that satisfies the decay condition of [1] only across a discretized grid over the bounded input space. BFComp then appeals to the δ-decidability-based dReal [6] to verify that the decay requirement, which is encoded by the SMT formula ψ, is exhaustively satisfied over the exterior of the CBF's l-level set.

Level sets are used here because dReal relies fundamentally on the technique of δ-relaxation, which may lead to spurious counterexamples. The parameter l is (iteratively) tuned to filter the domain of ψ to avoid such counterexamples. A positive result by dReal implies that the CBF is actually a valid BF everywhere outside the l-level set. If a (genuine) counterexample $\mathbf{c} = (\mathbf{x}_1, \mathbf{x}_2, u_1, u_2)$ to ψ is found, then $\mathbf{c}$ is used to refine the input-space grid.

To illustrate the utility of BFComp, we apply it to the model-order reduction of a canonical cardiac-cell model [19]. In particular, we use our framework to compute BFs that appeal to the small-gain theorem of [1] to establish that the four-variable Markovian potassium-channel component of the cell model can be safely replaced by an approximately equivalent one-variable abstraction. The canonical model captures the feedback-based interconnection of the four-variable model within the detailed 67-variable Iyer-Mazhari-Winslow (IMW) ventricular cell model [30]. To the best of our knowledge, this is the first compositional proof of a feedback-based approximate model-order reduction of a biological system.

The rest of the paper develops along the follow lines. Section 2 reviews basic definitions and properties of BFs from [1], our previous work on SOSP 1 [19], and the four-variable potassium channel model from [30]. Section 3 discusses the one-variable potassium channel abstraction. Section 4 describes our BF-based approach to establishing the substitutivity result within the canonical cell model. Section 5 presents SOSP 2, while Section 6 considers our dReal-based validation of SOSP 1 CBFs. Section 7 presents the results of our case study and highlights the implementation issues we faced with BFComp. Section 8 considers related work. Section 9 contains our concluding remarks and directions for future work.

2. BACKGROUND

In this section, we review the results on BFs from [1] and our input-space sampling-based algorithm from [19]. Then, we present physiological background by introducing the four-variable Markovian subsystem for the I_{Ks} current of the IMW model.

We define dynamical systems using a 6-tuple $(\mathcal{X}, \mathcal{X}^0, \mathcal{U}, f, \mathcal{O}, g)$, where $\mathcal{X}$ is the *state space*, $\mathcal{X}^0 \subseteq \mathcal{X}$ is the set of *initial conditions*, $\mathcal{U}$ is the *input space*, $f : \mathcal{X} \times \mathcal{U} \to \mathcal{X}$ is the *vector field* defining the dynamics, $\mathcal{O}$ is the set of *outputs*, and $g : \mathcal{X} \to \mathcal{O}$ maps a state to its output.

2.1 Bisimulation Functions

BFs [1] are contractive functions that characterize the joint IOS of two dynamical systems. The following definition is adapted from [1] and uses $\| \, . \, \|$ to denote the squared L2-norm.

Definition 1. Let $\Sigma_i = (\mathcal{X}_i, \mathcal{X}_i^0, \mathcal{U}, f_i, \mathcal{Y}, g_i)$, $i = 1, 2$, be two dynamical systems such that $\mathcal{X}_i \subseteq \mathbb{R}^{n_i}$, $\mathcal{U} \subseteq \mathbb{R}^m$ and $\mathcal{Y} \subseteq \mathbb{R}^p$. A *bisimulation function* (BF) is a smooth function $S : \mathbb{R}^{n_1} \times \mathbb{R}^{n_2} \to \mathbb{R}_{\geq 0}$ such that for every $\mathbf{x}_1 \in \mathcal{X}_1$, $\mathbf{x}_2 \in \mathcal{X}_2$, $\mathbf{u}_1, \mathbf{u}_2 \in \mathcal{U}$:

$$\| \, g_1(\mathbf{x}_1) - g_2(\mathbf{x}_2) \, \| \leq S(\mathbf{x}_1, \mathbf{x}_2), \tag{1}$$

$$\exists \lambda > 0, \gamma \geq 0 \text{ such that } \forall \mathbf{x}_1, \mathbf{x}_2, \mathbf{u}_1, \mathbf{u}_2 :$$
$$\frac{\partial S}{\partial \mathbf{x}_1} f_1(\mathbf{x}_1, \mathbf{u}_1) + \frac{\partial S}{\partial \mathbf{x}_2} f_2(\mathbf{x}_2, \mathbf{u}_2) \leq -\lambda \, S(\mathbf{x}_1, \mathbf{x}_2) + \gamma \, \| \, \mathbf{u}_1 - \mathbf{u}_2 \, \| \tag{2}$$

Next, we present a modified version of Theorem 1 of [1], which captures the joint IOS of two systems.

Theorem 1. Let S be a BF with parameters λ and γ between dynamical systems Σ_i, $i = 1, 2$, and let $\mathbf{x}_1(t)$ and $\mathbf{x}_2(t)$ be two trajectories of the systems. For all $t \geq 0$,

$$\begin{aligned} \| \, g_1(\mathbf{x}_1(t)) - g_2(\mathbf{x}_2(t)) \, \| &\leq S(\mathbf{x}_1(t), \mathbf{x}_2(t)) \\ &\leq e^{-\lambda t} S(\mathbf{x}_1(0), \mathbf{x}_2(0)) + \frac{\gamma}{\lambda} \, \| \, \mathbf{u}_1 - \mathbf{u}_2 \, \|_\infty \end{aligned}$$

where $\| \, \mathbf{u}_1 - \mathbf{u}_2 \, \|_\infty = sup_{t \geq 0} \, \| \, \mathbf{u}_1(t) - \mathbf{u}_2(t) \, \|$ denotes the maximum difference in the input signals being fed to the two systems.

PROOF. See the supplementary document [18]. □

The *feedback composition* $\Sigma_A || \Sigma_B$ of two dynamical systems Σ_A and Σ_B is obtained by feeding the output of Σ_A as the input to Σ_B and vice versa. When subsystems are connected using feedback, their respective BFs can be composed subject to a small-gain condition. We formalize this idea by stating a result based on Theorem 2 of [1].

Theorem 2. Let $\Sigma_i = (\mathcal{X}_i, \mathcal{X}_i^0, \mathcal{U}_i, f_i, \mathcal{O}_i, g_i)$, $i = 1, 2, A, B$, be dynamical systems such that $\mathcal{U}_1 = \mathcal{O}_A$, $\mathcal{U}_A = \mathcal{O}_1$, $\mathcal{U}_2 = \mathcal{O}_B$ and $\mathcal{U}_B = \mathcal{O}_2$. Let S_{12}, parameterized by λ_{12} and γ_{12}, be a BF between Σ_1 and Σ_2. Let S_{AB}, parameterized by λ_{AB} and γ_{AB}, be a BF between Σ_A and Σ_B.

Let $\Sigma_{A1} = \Sigma_A || \Sigma_1$ and $\Sigma_{B2} = \Sigma_B || \Sigma_2$. If the *small-gain condition* (SGC) $\frac{\gamma_{AB}\gamma_{12}}{\lambda_{AB}\lambda_{12}} < 1$ is met, then a BF S can be constructed between Σ_{A1} and Σ_{B2} by composing S_{AB} and S_{12} as follows:

$$S(\mathbf{x}_{A1}, \mathbf{x}_{B2}) = \alpha_1 S_{AB}(\mathbf{x}_A, \mathbf{x}_B) + \alpha_2 S_{12}(\mathbf{x}_1, \mathbf{x}_2) \tag{3}$$

where $\mathbf{x}_{A1} = [\mathbf{x}_A, \mathbf{x}_1]^T$ and $\mathbf{x}_{B2} = [\mathbf{x}_B, \mathbf{x}_2]^T$ and the constants α_1 and α_2 are given by:

$$\begin{cases} \frac{\gamma_{12}}{\lambda_{AB}} < \alpha_1 < \frac{\lambda_{12}}{\gamma_{AB}} \quad \text{and} \quad \alpha_2 = 1 \quad \text{if} \quad \lambda_{AB} \leq \gamma_{12} \\ \alpha_1 = 1 \quad \text{and} \quad \frac{\gamma_{AB}}{\lambda_{12}} < \alpha_2 < \frac{\lambda_{AB}}{\gamma_{12}} \quad \text{if} \quad \lambda_{12} \leq \gamma_{AB} \\ \alpha_1 = 1 \quad \text{and} \quad \alpha_2 = 1 \quad \text{in other cases} \end{cases} \tag{4}$$

PROOF. See the supplementary document [18]. □

2.2 Computing CBFs using SOS Optimization and Input-Space Sampling

In [19], we presented SOSP 1, a computation procedure based on SOS optimization for computing CBFs. In this subsection, we review the algorithm and comment on its input-space sampling approach.

A multivariate polynomial $p(x_1, x_2, \ldots, x_n) = p(\mathbf{x})$ is an *SoS polynomial* if there exist polynomials $f_1(\mathbf{x}), \ldots, f_m(\mathbf{x})$ such that $p(\mathbf{x}) = \sum_{i=1}^m f_i^2(\mathbf{x})$. For example, $p(x, y) = x^2 - 6xy + 12y^2$ is an SoS polynomial; it can be expressed as $(x-3y)^2 + (\sqrt{3}y)^2$. We denote the set of all SoS polynomials by $\mathbb{S}$.

An *SOS optimization Problem* (SOSP), involves finding an $S \in \mathbb{S}$ such that a linear objective function, whose decision variables are the coefficients of S, is optimized. The constraints of the problem are linear in the decision variables. A formal definition of an SOSP can be found in the SOSTOOLS user guide (p. 7).

Consider two dynamical systems $(X_i, \{\mathbf{x}_i^0\}, [u_{min}, u_{max}], f_i, O, g_i)$, $i = 1, 2$, with u_1 and u_2 being the scalar inputs to the two systems. Let $\mathcal{U}^G$ represent a discretized grid for u_1 and u_2. The grid is formed by dividing input space $[u_{min}, u_{max}]$ into a finite number of uniformly spaced intervals, and (u_1^i, u_2^j) denotes the pair of inputs where u_1 takes the i^{th} value and u_2 takes the j^{th} value. In [19], we presented the following SOSP for computing BFs using SOS optimization.

Definition 2. SOSP 1, as per [19], is defined by the following equations.

$$\text{Minimize } S(\mathbf{x}_1^0, \mathbf{x}_2^0) \tag{5}$$

subject to:

$$-S(\mathbf{x}_1, \mathbf{x}_2) + [g_1(\mathbf{x}_1) - g_2(\mathbf{x}_2)]^2 \in \mathbb{S}, \tag{6}$$

$$\exists \lambda > 0, \gamma \geq 0 \text{ such that } \forall \mathbf{x}_1, \mathbf{x}_2, u_1^i \in \mathcal{U}^G, u_2^j \in \mathcal{U}^G : \tag{7}$$
$$-\frac{\partial S}{\partial \mathbf{x}_1} f_1(\mathbf{x}_1, u_1^i) - \frac{\partial S}{\partial \mathbf{x}_2} f_2(\mathbf{x}_2, u_2^j) - \lambda S(\mathbf{x}_1, \mathbf{x}_2) + \gamma (u_1^i - u_2^j)^2 \in \mathbb{S}.$$

The CBF S starts at its maximum value at the pair of initial conditions $(\mathbf{x}_1^0, \mathbf{x}_2^0)$, and then decays along various trajectories of the two systems. Thus, along any pair of trajectories, the gap between $S(\mathbf{x}_1(t), \mathbf{x}_2(t))$ and the Squared Output Difference (SOD) $[g_1(\mathbf{x}_1(t)) - g_2(\mathbf{x}_2(t))]^2$ is maximum at $t = 0$,

i.e. at the initial states. To improve the bound on the SOD given by S, we minimized $S(\mathbf{x}_1(0), \mathbf{x}_2(0))$ as the objective function of the SOSP.

Eq. (7) enforces the decay condition for a BF, given by Eq. (2), only on the samples (u_1^i, u_2^j) that comprise the grid $\mathcal{U}$. The validity of Eq. 2 on the entire input space can be verified using delta-decidability, as shown in Sec. 6. In Sec. 5, we present an alternative SOSP that enforces Eq. (2) on the entire input space.

Next, we introduce the detailed Markovian potassium-channel model, which is employed as a component in the Iyer-Mazhari-Winslow (IMW) ventricular myocyte model [30].

2.3 The Potassium-Channel Subsystem

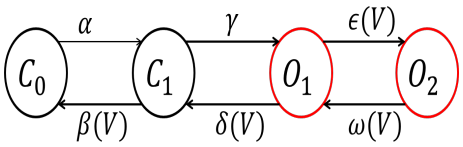

Figure 2: Σ_K: the detailed potassium-channel model, corresponding to the ionic current I_{Ks} in the IMW model.

Definition 3. The *potassium channel model* Σ_K is given by $(X, X^0, \mathcal{V}, f_K, \mathcal{O}, g_K)$. A *state* $\mathbf{x} \in X \subseteq \mathbb{R}^4_{\geq 0}$ is the occupancy probability distribution over the four states of the voltage-controlled Continuous Time Markov Chain (CTMC) shown in Fig. 2 in the following order of the state labels: $[C_0, C_1, O_1, O_2]$. The dynamics f_K is given by

$$f_K : \dot{\mathbf{x}} = A_K(V)\ \mathbf{x}, \tag{8}$$

where $V \in \mathcal{V} \subseteq \mathbb{R}$, the transmembrane voltage, is the input to the system and $A_K(V)$ is the 4×4 voltage-controlled rate matrix. The off-diagonal entry $A_K(i,j), i \neq j$, is the transition rate from state $\mathbf{x}_j$ to state $\mathbf{x}_i$. For example, $A_I(3,4) = \omega(V)$, the transition rate from O_2 to O_1. The diagonal entry $A_I(i,i)$ is the sum of all the outgoing rates from state $\mathbf{x}_i$. The transition rates are as follows.

$$\begin{aligned}
\alpha &= 7.956 \times 10^{-3} \\
\beta(V) &= 0.216 \times exp(-0.00002\ V) \\
\gamma &= 3.97 \times 10^{-2} \\
\delta(V) &= (7 \times 10^{-3}) \times exp(-0.15\ V) \\
\epsilon(V) &= (7.67 \times 10^{-3}) \times exp(0.087\ V) \\
\omega(V) &= (3.8 \times 10^{-3}) \times exp(-0.014\ V)
\end{aligned}$$

The set of outputs $\mathcal{O} \subseteq \mathbb{R}_{\geq 0}$ contains the conductance values for the states. Given a state $\mathbf{x}$, $g_K(\mathbf{x}) \triangleq \mathbf{x}_3 + \mathbf{x}_4$ maps it to its conductance given by the sum of the occupancy probabilities of the states labeled O_1 and O_2. The system has a single initial condition $\mathbf{x}_0 = [0.9646, 0.03543, 2.294 \times 10^{-7}, 4.68 \times 10^{-11}] \in X^0$, as per Table 4 of [30].

In Section 3, we show that a one-variable approximation for Σ_K can be identified using our curve-fitting-based approach of [2, 12].

3. MODEL-ORDER REDUCTION OF Σ_K

The curve fitting-based approach of [2, 12] can be used to identify the following one-variable Hodgkin Huxley (HH)-type approximation for Σ_K.

Definition 4. The *HH-type abstraction* Σ_H is given by $(Y, Y^0, \mathcal{V}, f_H, \mathcal{O}, g_H)$. A *state* $\mathbf{y} \in Y \subseteq \mathbb{R}_{\geq 0}$ denotes the value of an activating (m-type) subunit. The dynamics f_H is given by

$$f_H : \dot{y} = \alpha_m(V)(1 - y) - \beta_m(V)y, \tag{9}$$

where $V \in \mathcal{V} \subseteq \mathbb{R}$, the transmembrane voltage, is the input to the system. The rate functions $\alpha_m(V)$ and $\beta_m(V)$, identified using the two-step curve fitting-based approach of [2, 12], are as follows.

$$\begin{aligned}
\alpha_m(V) = {} & (-1.331 \times 10^{-10})V^4 - (2.466 \times 10^{-7})V^3 \\
& - (9.723 \times 10^{-6})V^2 - 0.0001231V + 0.001049
\end{aligned} \tag{10}$$

$$\begin{aligned}
\beta_m(V) = {} & (4.788 \times 10^{-10})V^6 - (1.547 \times 10^{-8})V^5 \\
& + (1.642 \times 10^{-7})V^4 - (2.85 \times 10^{-6})V^3 \\
& + (6.704 \times 10^{-5})V^2 - (0.0007041)V + 0.003285
\end{aligned} \tag{11}$$

The set of outputs $\mathcal{O} \subseteq \mathbb{R}_{\geq 0}$ contains the conductance values for the states. Given a state $\mathbf{y}$, $g_H(y) \triangleq y$ maps it to its conductance. The system has a single initial condition $y_0 = 1.32 \times 10^{-5}$.

4. CANONICAL CELL MODELS AND COMPOSITIONAL REASONING

In this section, we setup our case study on approximate model-order reduction within feedback loops. We first introduce the voltage subsystem Σ_C representing the cell membrane, which we compose with Σ_K and Σ_H to obtain two *Canonical Cell Models* (CCMs). We then state our compositionality result in terms of the two CCMs, and show how BFs can be used to prove the result.

Definition 5. The *voltage subsystem* Σ_C is a capacitor-like model given by $(\mathcal{V}, \mathcal{V}^0, \mathcal{O}, f_C, \mathcal{V}, g_C)$. State $V \in \mathcal{V} \subseteq \mathbb{R}$ is the voltage. The dynamics of Σ_C is given by

$$f_C : \dot{V} = -G_K(V - E_K)\ O \tag{12}$$

where $G_K = 90.58$ and $E_K = -35\ mV$ are the parameters of the model, and $O \in \mathcal{O} \subseteq \mathbb{R}_{\geq 0}$, the conductance of the potassium channel, is Σ_C's input. The system outputs its state, i.e., for $V \in \mathcal{V}$, $g_C(V) = V$, and the initial condition is $V_0 = 0\ mV$.

As per Eq. (12), V_{Na} represents the equilibrium for a fixed-conductance input. Thus, V takes values in $[-35,\ 0]$.

In the case of detailed cardiac cell models, such as the IMW model, ion-channel subsystems such as Σ_K and Σ_H take voltage as input from the rest of the model and provide the conductance of the channel as the output. The rest of the model takes the channel conductance as input and outputs the voltage, which is then fed back to the ion-channel subsystems. Next, we define CCMs Σ_{CK} and Σ_{CH} that reflect this feedback-based composition. The models are canonical in the sense that other ion-channel subsystems can be similarly added to obtain a complete IMW model.

Definition 6. Systems Σ_{CK} and Σ_{CH} (see Fig. 3) are obtained by performing feedback-composition on the voltage subsystem Σ_C with ion-channel subsystems Σ_K and Σ_H, respectively; i.e., $\Sigma_{CK} = \Sigma_C||\Sigma_K$ and $\Sigma_{CH} = \Sigma_C||\Sigma_H$. The state spaces, initial conditions, dynamics and outputs are inherited from the subsystems, as explained below. Both Σ_{CK} and Σ_{CH} are autonomous systems and do not receive any external inputs.

A state of Σ_{CK} is given by $[\mathbf{x}, V_K]^T$, where $\mathbf{x}$ is a state of Σ_K and V_K is a state of Σ_C. The subscript K in V_K is used to denote the copy of Σ_C composed with Σ_K. The system dynamics are given by Eqs. (8) and (12). The output is given by $[g_K(\mathbf{x}), V_K]^T$. The initial condition is the pair of the initial conditions of Σ_K and Σ_C.

A state of Σ_{CH} is given by $[y, V_H]^T$, where y denotes a state of Σ_H and V_H denotes a state of Σ_C. The subscript H in V_H is used to denote the copy of Σ_C composed with Σ_H. The system dynamics are given by Eqs. (9) and (12). The output is given by $[g_H(y), V_H]^T$. The initial condition is the pair of the initial conditions of Σ_H and Σ_C.

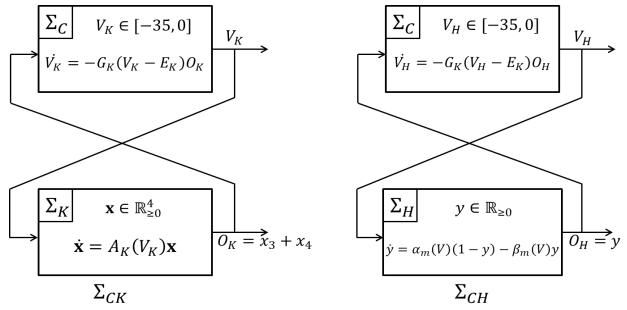

Figure 3: Σ_{CK} and Σ_{CH}: ion-channel subsystems Σ_K and Σ_H are feedback-composed with Σ_C, which represents the cell membrane. Σ_{CH} is obtained by i) identifying the one-variable abstraction Σ_H of Σ_K using the curve-fitting procedure given in [2, 12]; and ii) substituting Σ_H for the detailed model Σ_K within Σ_{CK}.

When Σ_K in Σ_{CK} is substituted for by Σ_H to obtain Σ_{CH}, the behaviors of the composite CCMs might diverge. This is due to the feedback composition that tends to amplify deviations in the outputs of either of the subsystems. Fig. 4 shows a pair of trajectories of Σ_{CK} and Σ_{CH} that start from nominal initial conditions. The goal of the paper is to compute BFs that show that the composite CCMs are indeed approximately equivalent, i.e., the following statement is valid.

Compositionality Result: There exists a BF S between Σ_{CK} and Σ_{CH} that renders the two CCMs to be approximately equivalent in the sense characterized by Theorem 1.

S is computed compositionally as follows. First, the components Σ_K and Σ_H are proved to be approximately equivalent by computing a BF S_{KH} between the two systems. Then, the context Σ_C is proved to be robust to input deviations by computing a BF S_C for it. The computation procedure ensures that the prerequisite small-gain condition is satisfied by S_{KH} and S_C, thereby enabling the application of Theorem 2; this results in a BF S between Σ_{CK} and Σ_{CH}. We

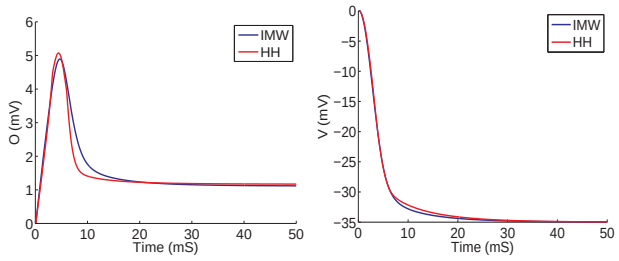

(a) $O_K(t)$ and $O_H(t)$ of Σ_{CK} and Σ_{CH} respectively. (b) $V_K(t)$ and $V_H(t)$ of Σ_{CK} and Σ_{CH} respectively.

Figure 4: Simulations of Σ_{CK} and Σ_{CH}: when Σ_K is replaced by Σ_H, feedback composition tends to accumulate error incurred due to the abstract component. The mean L1 errors: O_{Ks} : 1.1786×10^{-4}, V: $0.2002\ mV$.

describe the automated framework for computing S_{KH} and S_C in the following sections.

5. COMPUTING BFs USING SOS OPTIMIZATION

In this section, we describe SOSP 2, an SOSP formulation that can be used to compute BFs. SOSP 2, in contrast to SOSP 1, which was reviewed in Section 2.2, exhaustively covers the input-space. We begin by presenting the problem formulation, and then, we show that the solutions are indeed BFs.

We assume that the input spaces are described using sets, such as $\mathcal{U} = \{u \in \mathbb{R} : \rho(u) \geq 0\}$, where $\rho(u)$ is called a *descriptor function*. For example, $\rho(u) = (u - u_{min})(u_{max} - u)$ describes the input-space $\mathcal{U} = [u_{min}, u_{max}]$. We denote the components of the state vectors as $\mathbf{x}_1 = [x_{11}, x_{12}, \ldots, x_{1n_1}]$ and $\mathbf{x}_2 = [x_{21}, x_{22}, \ldots, x_{2n_2}]$. Each of these components take values in a closed interval, i.e. $x_{11} \in [\underline{x_{11}}, \overline{x_{11}}], \ldots, x_{1n_1} \in [\underline{x_{1n_1}}, \overline{x_{1n_1}}]$ and $x_{21} \in [\underline{x_{21}}, \overline{x_{21}}], \ldots, x_{2n_2} \in [\underline{x_{2n_2}}, \overline{x_{2n_2}}]$. We introduce vectors of polynomials τ_1 and τ_2 as descriptor functions of the state vectors:

$$\tau_i(\mathbf{x}_i) = \begin{bmatrix} (x_{i1} - \underline{x_{i1}})(\overline{x_{i1}} - x_{i1}) \\ \vdots \\ (x_{in_i} - \underline{x_{in_i}})(\overline{x_{in_i}} - x_{in_i}) \end{bmatrix}, i = 1, 2. \quad (13)$$

Definition 7. Consider two dynamical systems $\Sigma_i = (X_i, \{\mathbf{x}_i^0\}, [u_{min}, u_{max}], f_i, \mathcal{O}, g_i)$, $i = 1, 2$. SOSP 2 is given by the following equations.

$$\text{Minimize } S(\mathbf{x}_1^0, \mathbf{x}_2^0) \quad (14)$$

subject to:

$$-S(\mathbf{x}_1, \mathbf{x}_2) + [g_1(\mathbf{x}_1) - g_2(\mathbf{x}_2)]^2 \in \mathbb{S}, \quad (15)$$

$\forall u_i \in [u_{min}, u_{max}], x_{ij} \in [\underline{x_{ij}}, \overline{x_{ij}}], i = 1, 2, j = 1, \ldots, n_i,$

$\exists \lambda > 0, \gamma \geq 0, \sigma_1(\mathbf{x}_1, u_1) \in \mathbb{S}, \sigma_2(\mathbf{x}_2, u_2) \in \mathbb{S}$, and vectors of SOS polynomials $\sigma_3(\mathbf{x}_1, u_1)$ and $\sigma_4(\mathbf{x}_2, u_2)$ such that :

$$-\frac{\partial S}{\partial \mathbf{x}_1} f_1(\mathbf{x}_1, u_1) - \frac{\partial S}{\partial \mathbf{x}_2} f_2(\mathbf{x}_2, u_2) - \lambda S(\mathbf{x}_1, \mathbf{x}_2) + \gamma(u_1 - u_2)^2 - \sigma_1(\mathbf{x}_1, u_1)\rho(u_1) - \sigma_2(\mathbf{x}_2, u_2)\rho(u_2) - \sigma_3(\mathbf{x}_1, u_1)\tau_1(\mathbf{x}_1) - \sigma_4(\mathbf{x}_2, u_2)\tau_2(\mathbf{x}_2) \in \mathbb{S}. \quad (16)$$

Next, we show that the feasible solutions of SOSP 2 are indeed BFs for the two systems.

Theorem 3. Consider a feasible solution, $(S, \sigma_1, \sigma_2, \sigma_3, \sigma_4, \lambda, \gamma)$, of the SOSP 2. S satisfies Eqs. (1) and (2), and thus is a BF between Σ_1 and Σ_2.

PROOF. S, from a feasible solution $(S, \sigma_1, \sigma_2, \sigma_3, \sigma_4\lambda, \gamma)$, satisfies Eq. (15):

$$\forall \mathbf{x}_1, \mathbf{x}_2 : -S(\mathbf{x}_1, \mathbf{x}_2) + [g_1(\mathbf{x}_1) - g_2(\mathbf{x}_2)]^2 \in \mathbb{S}.$$

As an SOS polynomial is always non-negative, we get

$$-S(\mathbf{x}_1, \mathbf{x}_2) + [g_1(\mathbf{x}_1) - g_2(\mathbf{x}_2)]^2 \geq 0,$$

which implies $[g_1(\mathbf{x}_1) - g_2(\mathbf{x}_2)]^2 \leq -S(\mathbf{x}_1, \mathbf{x}_2)$, i.e. S satisfies Eq. (1).

A feasible solution satisfies Eq. (16):

$$\begin{aligned}
&-\frac{\partial S}{\partial \mathbf{x}_1} f_1(\mathbf{x}_1, u_1) - \frac{\partial S}{\partial \mathbf{x}_2} f_2(\mathbf{x}_2, u_2) - \lambda S(\mathbf{x}_1, \mathbf{x}_2) + \gamma(u_1 - u_2)^2 \\
&- \sigma_1(\mathbf{x}_1, u_1)\rho(u_1) - \sigma_2(\mathbf{x}_2, u_2)\rho(u_2) - \sigma_3(\mathbf{x}_1, u_1)\tau_1(\mathbf{x}_1) \\
&- \sigma_4(\mathbf{x}_2, u_2)\tau_2(\mathbf{x}_2) \in \mathbb{S}.
\end{aligned}$$

Non-negativity of SOS polynomials leads to

$$\begin{aligned}
&-\frac{\partial S}{\partial \mathbf{x}_1} f_1(\mathbf{x}_1, u_1) - \frac{\partial S}{\partial \mathbf{x}_2} f_2(\mathbf{x}_2, u_2) - \sigma_1(\mathbf{x}_1, u_1)\rho(u_1) \\
&- \sigma_2(\mathbf{x}_2, u_2)\rho(u_2) - \sigma_3(\mathbf{x}_1, u_1)\tau_1(\mathbf{x}_1) - \sigma_4(\mathbf{x}_2, u_2)\tau_2(\mathbf{x}_2) \\
&\geq \lambda S(\mathbf{x}_1, \mathbf{x}_2) - \gamma(u_1 - u_2)^2.
\end{aligned}$$

Multiplying both sides by -1 and then reversing the inequality, we get

$$\begin{aligned}
&\frac{\partial S}{\partial \mathbf{x}_1} f_1(\mathbf{x}_1, u_1) + \frac{\partial S}{\partial \mathbf{x}_2} f_2(\mathbf{x}_2, u_2) + \sigma_1(\mathbf{x}_1, u_1)\rho(u_1) \\
&+ \sigma_2(\mathbf{x}_2, u_2)\rho(u_2) + \sigma_3(\mathbf{x}_1, u_1)\tau_1(\mathbf{x}_1) + \sigma_4(\mathbf{x}_2, u_2)\tau_2(\mathbf{x}_2) \\
&\leq -\lambda S(\mathbf{x}_1, \mathbf{x}_2) + \gamma(u_1 - u_2)^2.
\end{aligned}$$

As $\sigma_1(\mathbf{x}_1, u_1)\rho(u_1) + \sigma_2(\mathbf{x}_2, u_2)\rho(u_2) + \sigma_3(\mathbf{x}_1, u_1)\tau_1(\mathbf{x}_1) + \sigma_4(\mathbf{x}_2, u_2)\tau_2(\mathbf{x}_2)$ is always non-negative, we can eliminate the sum and still retain the inequality to get

$$\frac{\partial S}{\partial \mathbf{x}_1} f_1(\mathbf{x}_1, u_1) + \frac{\partial S}{\partial \mathbf{x}_2} f_2(\mathbf{x}_2, u_2) \leq -\lambda S(\mathbf{x}_1, \mathbf{x}_2) + \gamma(u_1 - u_2)^2.$$

□

6. VALIDATING SOSP 1 BFs USING DELTA-DECIDABILITY

Consider the two dynamical systems $(X_i, \{\mathbf{x}_i^0\}, [u_{min}, u_{max}], f_i, O, g_i)$, $i = 1, 2$. Let S, parameterized by λ and γ, be a CBF, which can be obtained by solving SOSP 1, see Def. 2. A valid solution of SOSP 1 satisfies Eq. (2) over the input grid $\mathcal{U}^G$ that is used in SOSP 1. The focus of this section is to validate if S satisfies Eq. (2) over all the states and inputs, and thus is a BF for the two systems. For this purpose, we use dReal [6], which implements delta-decidability, to validate S. We begin by defining the function ψ as

$$\begin{aligned}
\psi(\mathbf{x}_1, \mathbf{x}_2, u_1, u_2) \triangleq &-\frac{\partial S}{\partial \mathbf{x}_1} f_1(\mathbf{x}_1, u_1) - \frac{\partial S}{\partial \mathbf{x}_2} f_2(\mathbf{x}_2, u_2) \\
&- \lambda S(\mathbf{x}_1, \mathbf{x}_2) + \gamma(u_1 - u_2)^2.
\end{aligned}$$

If S satisfies Eq. (2) over the entire state and input space, then the following SMT formula must be unsatisfiable:

$$\exists \mathbf{x}_1, \mathbf{x}_2, u_1, u_2 : \psi(\mathbf{x}_1, \mathbf{x}_2, u_1, u_2) < 0 \tag{17}$$

Delta-decidability, which involves relaxing ψ by a parameter $\delta > 0$, can be used to check if Eq. (17) is indeed unsatisfiable. The open-source tool *dReal* implements δ-decision procedures and can be used for our problem. A decision procedure is said to be δ-complete if for any SMT formula, it returns either *unsat*, if the formula is unsatisfiable, or returns *δ-sat*, if the formula's δ-relaxation is satisfiable, see [6, 4, 5] for a formal definition.

When Eq. (17) is presented to dReal, with a pre-determined δ, three possibilities, which are illustrated in Fig. 5, arise. We discuss each of them next.

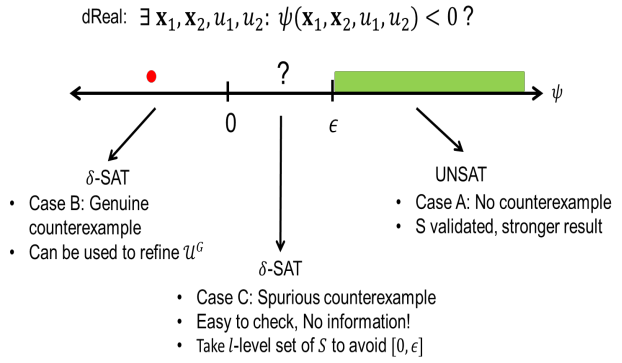

Figure 5: Validating SOSP 1-based CBFs using dReal.

Case A, dReal returns unsat: Eq. (17) is unsatisfiable, and therefore S is a valid BF. Delta-relaxation ensures a stronger result, we may claim that $\psi \geq \epsilon$, where ϵ is a function of δ and other internal parameters of dReal.

Case B, dReal returns δ-sat, with a counterexample, where $\psi < 0$. The tuple of states and inputs that is returned as the counterexample contains an input pair, where S fails to satisfy Eq. (2). The input pair is then used to refine $\mathcal{U}^G$ and SOSP 1 is repeated; Eq. (7), which represents a family of inequalities, is instantiated over $\mathcal{U}^G$, as well as the input pair from the counterexample.

Case C, dReal returns δ-sat, with a counterexample, where $\psi \geq 0$. This possibility arises due to the delta-relaxation. The formula ψ evaluates to a very small value in the range $[0, \epsilon]$. The counterexample is spurious and does not provide any information about S. Thus, we present a workaround to avoid this case.

To avoid Case C, we filter the domain of the state variables $\mathbf{x}_1$ and $\mathbf{x}_2$ in Eq. (17) to eliminate the pairs of states that contribute to the spurious counterexamples. Specifically, we validate the CBF S only on, and outside its l-level set. Eq. (17) is modified as

$$\exists \mathbf{x}_1, \mathbf{x}_2, u_1, u_2 : (S(\mathbf{x}_1, \mathbf{x}_2) \geq l) \wedge (\psi(\mathbf{x}_1, \mathbf{x}_2, u_1, u_2) < 0) \tag{18}$$

The intuition behind level-set-based filtering of the domain is as follows. The function ψ goes to 0 when the states and

the inputs go to 0. Also, ψ bounds the derivative of S with respect to time. The time-derivative of S takes very low values near the origin of the state-space, as the the origin is an equilibrium for our systems. Fig. 6 illustrates this property. When the inputs to the subsystem are held constant, the derivative of a BF becomes very low as the trajectories decay to the origin, which is a stable equilibrium. Thus, the derivative of S with respect to time, and consequently ψ, will have relatively larger values outside the l-level set of S.

The parameter l may be tuned till we avoid Case C completely and cover as many states as possible. Starting from an aggressive small value of $l \geq 0$, it may be incremented in small steps till Case C is completely avoided.

Our level-set-based approach can be justified as follows. We define the exterior of the l-level set of S as: $S^{\geq l} \triangleq \{(\mathbf{x}_1, \mathbf{x}_2) | \ S(\mathbf{x}_1, \mathbf{x}_2) \geq 0\}$. Validating Eq. (17) over $S^{\geq l}$ ensures that Eq. (1) and Eq. (2) are satisfied for all states within $S^{\geq l}$. In a practical setting, where we want to establish IOS between two systems, the sets of initial conditions become important. Given the decaying nature of a BF, the maximum value of the BF over a given pairing of the initial states is the best bound on the SOD that the BF can provide. Approximate bisimilarity of two systems can be established by minimizing the maximum value of the BF over all pairings of the initial states. For a given CBF, if this value is greater than the level set l, at which the CBF is validated, then the CBF can be used to be provide practical bounds on the SOD.

CBFs validated using the level-set-based approach also enable compositionality arguments, albeit in a weaker setting. To this end, we state the following proposition.

Proposition 1. Let $\Sigma_i = (\mathcal{X}_i, \mathcal{X}_i^0, \mathcal{U}_i, f_i, \mathcal{O}_i, g_i)$, $i = 1, 2$, A, B, be dynamical systems such that $\mathcal{U}_1 = \mathcal{O}_A$, $\mathcal{U}_A = \mathcal{O}_1$, $\mathcal{U}_2 = \mathcal{O}_B$ and $\mathcal{U}_B = \mathcal{O}_2$. Let S_{12}, parameterized by λ_{12} and γ_{12}, be a BF between Σ_1 and Σ_2 in $S_{12}^{\geq l_1}$. Let S_{AB}, parameterized by λ_{AB} and γ_{AB}, be a BF between Σ_A and Σ_B in $S_{AB}^{\geq l_2}$.

Let $\Sigma_{A1} = \Sigma_A || \Sigma_1$ and $\Sigma_{B2} = \Sigma_B || \Sigma_2$. If the *small gain condition* (SGC) $\frac{\gamma_{AB}\gamma_{12}}{\lambda_{AB}\lambda_{12}} < 1$ is met, then a BF S between Σ_{A1} and Σ_{B2}, which satisfies Eq. (1) and Eq. (2) over $S_{12}^{\geq l_1} \times S_{AB}^{\geq l_1}$, can be constructed as follows.

$$S(\mathbf{x}_{A1}, \mathbf{x}_{B2}) = \alpha_1 S_{AB}(\mathbf{x}_A, \mathbf{x}_B) + \alpha_2 S_{12}(\mathbf{x}_1, \mathbf{x}_2)$$

where $\mathbf{x}_{A1} = [\mathbf{x}_A, \mathbf{x}_1]^T$ and $\mathbf{x}_{B2} = [\mathbf{x}_B, \mathbf{x}_2]^T$ and the constants α_1 and α_2 are as per Theorem 2.

Proof. See supplementary document [18]. □

7. RESULTS

In this section, we elaborate on computing the BFs S_{KH}, S_C, and the composed BF S between Σ_{CK} and Σ_{CH} using our automated framework of Fig. 1. The BFs computed using SOSP 1 and SOSP 2 are then visualized along pairs of trajectories obtained by feeding constant-input signals to the corresponding systems.

7.1 Computing S_{KH} and S_C using SOSP 2

Automated solvers, such as MATLAB SOSTOOLS [24], which can be used to solve SOSP 2, have the following restriction: only polynomial vector fields, denoted by $f_i(\mathbf{x}_i, u_i)$, $i = 1, 2$ in Eq. (16), can be specified. In other words, f_i must be a polynomial function of $\mathbf{x}_i$ and u_i.

The potassium-channel subsystem Σ_K does not satisfy the above-mentioned requirement. The dynamics, see Eq. (8), is specified by $\dot{\mathbf{x}} = A_K(V).\mathbf{x}$, where $\mathbf{x}$ is the occupancy-probability vector and $A_K(V)$ is the rate matrix, whose entries are *exponential functions of the input membrane potential* V, see Defn. 3. Thus, the dynamics of Σ_K are not polynomial in the input.

As a workaround, we transformed the rate matrix $A_K(V)$ to an approximately equivalent matrix $A_K^p(V)$ by fitting the entries of A with polynomial functions using MATLAB *cftool* [20]. The polynomial approximations of the voltage-dependent rate functions, denoted by the superscript p are as follows.

$$\begin{aligned}
\beta^p(V) &= -(4.322e-6)V + 0.216, \\
\delta^p(V) &= (2.125e-010)V^6 - (9.322e-009)V^5 + \\
&\quad (8.964e-008)V^4 - (1.716e-006)V^3 + \\
&\quad (8.87e-005)V^2 - 0.001284V + 0.006744, \\
\epsilon^p(V) &= (4.435e-009)V^4 + (5.191e-007)V^3 + \\
&\quad (2.539e-005)V^2 + (0.0006507)V + 0.007652, \text{and} \\
\omega^p(V) &= (3.771e-007)V - (5.415e-005)V + 0.0038.
\end{aligned}$$

Computing S_{KH} and S_C using SOSP 2 begins with declaring the form of the BFs. We chose ellipsoidal forms using the `sossosvar` function provided by SOSTOOLS: $S_{KH}(\mathbf{x}, \mathbf{y}) = [\mathbf{x}, \mathbf{y}].Q_{KH}.[\mathbf{x}, \mathbf{y}]^T$ and $S_C(V_K, V_H)$ $= [V_K, V_H].Q_C.[V_K, V_H]^T$. Variables $\mathbf{x}, \mathbf{y}, V_I$, and V_H are declared using the `pvar` polynomial variable toolbox. The coefficients of the BFs, which form the decision variables of the SoS optimization problems, are contained in the positive semidefinite matrices Q_{KH} (4×4) and Q_C (2×2). We chose ellipsoidal forms, using the `sossosvar`, for the $\sigma(.,.)$ functions that strengthen the decay requirement in Eq. (16) of Defn. 7. The descriptor functions were obtained from the definitions Σ_K, Σ_H and Σ_C.

7.2 Computing S_{KH} and S_C using SOSP 1 and dReal

The details of implementing SOSP 1 in MATLAB SOSTOOLS can be found in Sec. 3 of [19]. We provide details on dReal-based validation of the CBFs.

For S_{KH}, $\mathcal{V} = [-35, -25, -15, -5, 0]$. $\mathcal{V} \times \mathcal{V}$ was used as the input grid to compute the CBF S_{KH} using SOSP 1. S_{KH} was parameterized by $\lambda_{KH} = 0.001$ and $\gamma_{KH} = 0.0001$. The CBF was validated as per Sec. 6; Eq. (18) was proved to be *unsat* in dReal by choosing $l = 0.001$.

For S_C, we considered $\mathcal{O} \times \mathcal{O}$ as the input grid, where $\mathcal{O} = [0.1, 0.2, 0.3, 0.4, 0.5, 0.6, 0.7, 0.8, 0.9, 1]$. S_C was param-

eterized by $\lambda_C = 0.001$ and $\gamma_C = 0.0001$. The CBF The CBF was validated as per Sec. 6; Eq. (18) was proved to be *unsat* in dReal by choosing $l = 1$.

7.3 Composing S_{KH} and S_C using the Small-Gain Theorem

The parameters of S_{KH} and S_C satisfy the SGC condition of Theorem 2, as $\frac{\gamma_{KH}\gamma_C}{\lambda_{KH}\lambda_C} = 0.01 < 1$ in both SOSP 1 and SOSP 2. Applying Theorem 2, we linearly composed S_{IH} and S_C to obtain $S = \alpha_1 S_{IH} + \alpha_2 S_C$, where $\alpha_1, \alpha_2 = 1$. S is a BF between the composite systems Σ_{CK} and Σ_{CH}. As per Theorem 2 of [1], the parameter λ of S can be calculated as

$$\lambda = min\left(\frac{\alpha_1\lambda_{KH} - \alpha_2\gamma_C}{\alpha_1}, \frac{\alpha_2\lambda_C - \alpha_1\gamma_{KH}}{\alpha_2}\right) = 0.0009.$$

7.4 Visualizing the BFs

Empirical validation of the BFs is provided by plotting them in 2D along the time axis. As the time proceeds in the same manner in both systems, the corresponding BF is plotted for the pair of states occurring at the same time along the trajectories of the systems. The SOD observed for the pair of states is also plotted in the same graph. The resulting plots show that the BFs bound the SOD and decay in time along the pairs of trajectories, as per Theorem 1.

Figs. 6 (a) - (c) show S_{KH} plotted along three pairs of trajectories of Σ_K and Σ_H. Each pair was generated by supplying a pair of constant voltage signals $(V_1(t), V_2(t))$ as inputs to Σ_K and Σ_H, respectively. The two subsystems were initialized as per Defs. 3 and 4, and simulated using MATLAB's *ODE45* solver. S_{KH} was then evaluated along the resulting pair of trajectories after shifting the origin to the equilibrium defined by $(V_1(t), V_2(t))$. In two cases, S_{KH} computed using SOSP 2 provides slightly better error bound than that of using SOSP 1.

S_C characterizes the ability of Σ_C to tolerate small changes in the input conductance signals. In the composite systems Σ_{CK} and Σ_{CH}, these signals are provided by subsystems Σ_K and Σ_H, and thus vary slightly due to the fitting errors incurred by the model-order reduction as described in Sec.3.

S_C is plotted in Figs. 6 (d) - (f) along three pairs of trajectories of Σ_C. Each pair of trajectories was generated by supplying constant conductance (input) signals ($O_1(t)$, $O_2(t)$). Σ_C was initialized at 0 mV and simulated using the Euler method. S_C was evaluated along the resulting trajectories after shifting the origin to the equilibrium, -35 mV (E_K). We observed that S_C computed using SOSP 1 gives a tighter SOD bound compared to SOSP 2.

CCMs Σ_{CK} and Σ_{CH} are autonomous dynamical systems and do not receive any external inputs. To visualize the composite BF S, we simulated Σ_{CK} and Σ_{CH} using the Euler method. Fig. 4 plots the trajectories obtained from these simulations. The corresponding conductance traces of Fig. 4(a) and the voltage traces of Fig. 4(b) empirically validate that the composed models are approximately equivalent as predicted by Theorem 2. BF S along this pair, and two other pairs of trajectories is plotted in Fig. 6 (g) - (i). The value of S is dominated by the value of S_C, as it bounds the squared difference of voltages and is much larger than S_{KH}, which bounds differences in probabilities. This is reasonable as voltage is the primary entity of interest when analyzing excitable cells. One could scale subsystem Σ_C such that its output lies in $[0, 1]$ and is thus comparable to the outputs of Σ_K/Σ_H. In all three cases, S computed using SOSP 1 performs much better than the one computed using SOSP 2.

8. RELATED WORK

Initial work on computing BFs, [7, 8, 9, 1, 13, 15], depended primarily on SOS optimization. SOS optimization has also played a crucial role in enabling the automated computation of other Lyapunov-like functions, such as Barrier Certificates [23, 22] and discrepancy functions [3, 11]. In [23, 15], the authors employ an SOSP 2-like approach, which is based on the S-Procedure of [31] and entails strengthening the Lyapunov-like inequalities over the region-of-interest in the state and input spaces.

Despite the success of the above-mentioned approaches, SOS-optimization-based techniques suffer from various drawbacks, such as numerical errors and choosing the forms of the unknown polynomials, which may be crucial for getting good SOD bounds. The *simulation-based approach* to analyzing stability of dynamical systems in [14], which is closely related to our work, addresses some of these issues. Simulation traces of a given dynamical system are used to compute so-called Candidate Lyapunov Functions (CLFs). The authors then use a SMT-based ensemble of tools, which includes dReal, to validate the decay requirements over level sets of the CLF. Our computation framework differs from the work of [14] in three ways. Firstly, we focus on BFs that characterize IOS of dynamical systems, whereas the authors focus on Lyapunov stability in [14]. Secondly, as shown in our case study, our framework places emphasis on SOD to enable bounding the error that is incurred when a detailed subsystem is replaced by an abstraction within a feedback loop. Lastly, our framework is completely based on Sum-of-Square optimization, whereas the authors use a Linear Programming (LP)-based approach to computing the CLFs.

LP-based computation of Lyapunov-like functions is a promising alternative to SOS optimization. In [26, 25], the authors present LP formulations, based on Handelman representations of polynomials, to compute Lyapunov functions. Consequently, the computation avoids semi-definite programming, which enables SOS optimization, and is therefore more robust to numerical errors. Incorporating such LP-based approaches into our framework is part of the future work.

9. CONCLUSIONS

We presented BFComp, an automated framework based on SOS optimization and δ-decidability over the reals for computing BFs that characterize IOS of dynamical systems and provide reasonable bounds on the SOD between the systems. We applied BFComp to compute BFs that appeal to a small-gain theorem, thereby compositionally showing that a detailed four-variable potassium-channel model can be safely replaced by an approximately equivalent one-variable abstraction within a feedback-composed system.

As future work, we plan to incorporate the SOD bound ex-

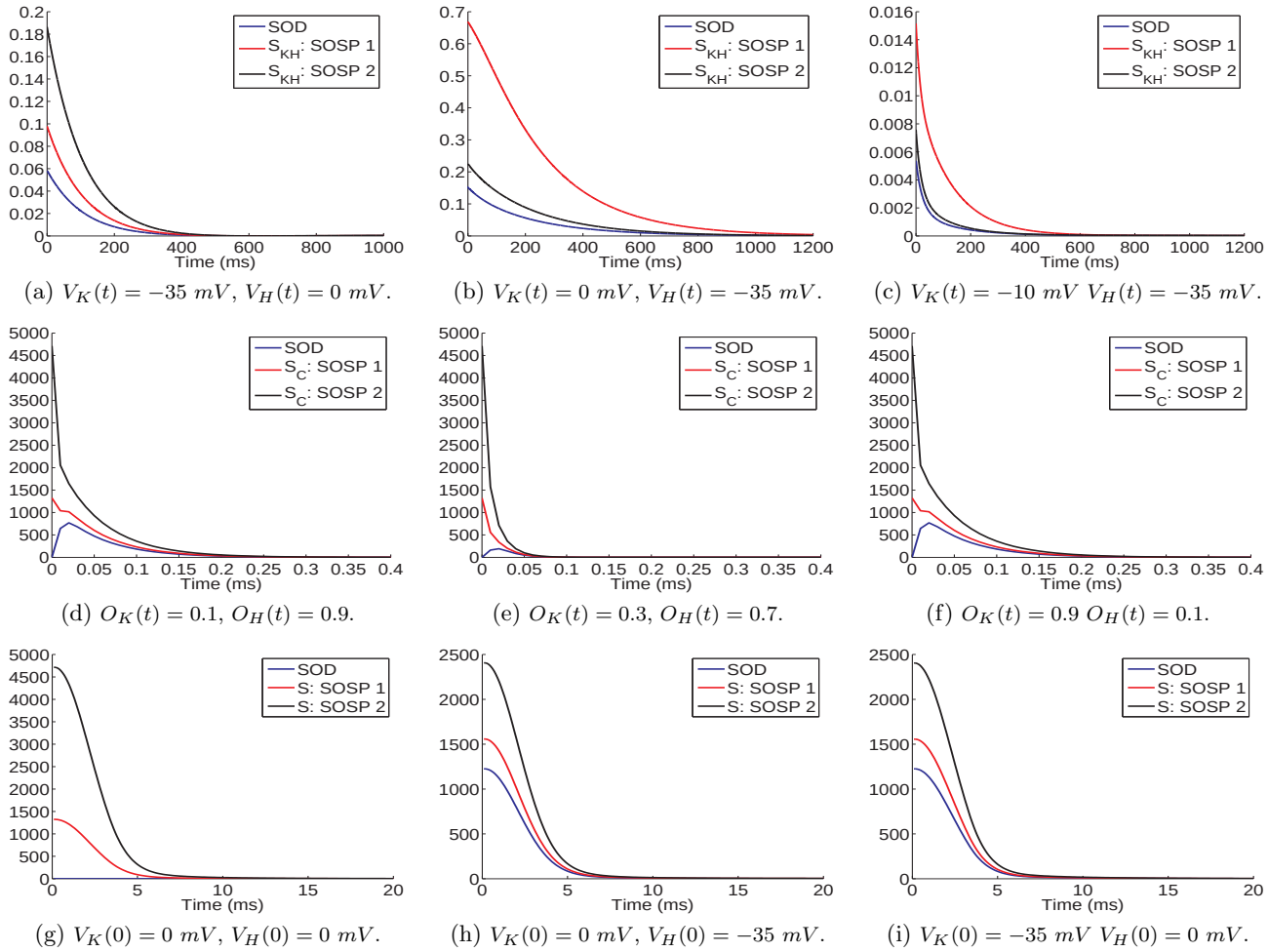

(a) $V_K(t) = -35\ mV$, $V_H(t) = 0\ mV$. (b) $V_K(t) = 0\ mV$, $V_H(t) = -35\ mV$. (c) $V_K(t) = -10\ mV$ $V_H(t) = -35\ mV$.

(d) $O_K(t) = 0.1$, $O_H(t) = 0.9$. (e) $O_K(t) = 0.3$, $O_H(t) = 0.7$. (f) $O_K(t) = 0.9$ $O_H(t) = 0.1$.

(g) $V_K(0) = 0\ mV$, $V_H(0) = 0\ mV$. (h) $V_K(0) = 0\ mV$, $V_H(0) = -35\ mV$. (i) $V_K(0) = -35\ mV$ $V_H(0) = 0\ mV$.

Figure 6: BFs S_{KH}, S_C, S, and their corresponding SOD plotted along trajectories of the respective systems. In subfigures (a) - (c), S_{KH} and SOD are plotted along three pairs of trajectories of Σ_K and Σ_H generated using constant voltage (input) signals. In subfigures (d) - (f), S_C and SOD are plotted along three pairs of trajectories of Σ_C generated using constant conductance (input) signals. In subfigures (g) - (h), the composed BF S and SOD are plotted along three pairs of trajectories of Σ_{CK} and Σ_{CH} generated using different initial conditions. In all three cases, the BFs upper bound the SOD and decay along the trajectories.

plicitly in BFComp, as a feedback that enables iterative improvement of the BFs. We will also investigate the LP-based approach of [25], which avoids semidefinite programming and is therefore more robust to numerical errors. Finally, we will seek to further generalize our small-gain theorem to enable compositional reasoning with CBFs that are guaranteed to satisfy the decay requirement over level sets, instead of the entire state and input spaces.

10. REFERENCES

[1] A. Girard. A composition theorem for bisimulation functions. *Pre-print*, 2007. arXiv:1304.5153.

[2] A. Murthy, M. A. Islam, E. Bartocci, E. Cherry, F. H. Fenton, J. Glimm, S. A. Smolka, and R. Grosu. Approximate bisimulations for sodium channel dynamics. In *Proceedings of CMSB'12, the 10th Conference on Computational Methods in Systems Biology*, LNCS, London, U.K., October 2012. Springer.

[3] P. S. Duggirala, S. Mitra, and M. Viswanathan. Verification of annotated models from executions. In *Proceedings of the Eleventh ACM International Conference on Embedded Software*, EMSOFT '13, pages 26:1–26:10, Piscataway, NJ, USA, 2013. IEEE Press.

[4] S. Gao, J. Avigad, and E. M. Clarke. Delta-complete decision procedures for satisfiability over the reals. In *Proceedings of the 6th International Joint Conference on Automated Reasoning*, IJCAR'12, pages 286–300, Berlin, Heidelberg, 2012. Springer-Verlag.

[5] S. Gao, J. Avigad, and E. M. Clarke. Delta-decidability over the reals. In *Proceedings of the 27th Annual IEEE Symposium on Logic in Computer Science (LICS), 2012*, pages 305–314. IEEE, 2012.

[6] S. Gao, S. Kong, and E. M. Clarke. dreal: An SMT solver for nonlinear theories over the reals. In *Automated Deduction–CADE-24*, pages 208–214. Springer, 2013.

[7] A. Girard and G. J. Pappas. Approximate

bisimulations for nonlinear dynamical systems. In *Proceedings of 44th IEEE Conference on Decision and Control*, Serville, Spain, December 2005.

[8] A. Girard and G. J. Pappas. Approximate bisimulation relations for constrained linear systems. *Automatica*, 43(8):1307 – 1317, August 2007.

[9] A. Girard and G. J. Pappas. Approximation metrics for discrete and continuous systems. *IEEE Transactions on Automatic Control*, 52(5):782 –798, May 2007.

[10] A. Girard and G. J. Pappas. Hierarchical control system design using approximate simulation. *Automatica*, 45(2):566 – 571, 2009.

[11] Z. Huang, C. Fan, A. Mereacre, S. Mitra, and M. Kwiatkowska. Invariant verification of nonlinear hybrid automata networks of cardiac cells. In *Proceedings of 26th International Conference on Computer Aided Verification (CAV)*, volume 8559 of *LNCS*, pages 373–390. Springer, 2014.

[12] M. A. Islam, A. Murthy, E. Bartocci, E. M. Cherry, F. H. Fenton, J. Glimm, S. A. Smolka, and R. Grosu. Model-order reduction of ion channel dynamics using approximate bisimulation. *Theoretical Computer Science*, 2014.

[13] A. A. Julius and G. J. Pappas. Approximate equivalence and approximate synchronization of metric transition systems. In *Proceedings of 45th IEEE Conference on Decision and Control*, San Diego, CA, 2006, December 2006.

[14] J. Kapinski, J. V. Deshmukh, S. Sankaranarayanan, and N. Arechiga. Simulation-guided Lyapunov analysis for hybrid dynamical systems. In *Hybrid Systems: Computation and Control (HSCC)*, pages 133–142. ACM Press, 2014.

[15] J. Kapinski, A. Donzé, F. Lerda, H. Maka, S. Wagner, and B. H. Krogh. Control software model checking using bisimulation functions for nonlinear systems. In *47th IEEE Conference on Decision and Control (CDC)*, pages 4024–4029, 2008.

[16] D. Liberzon. *Switching in Systems and Control*. Springer, 2003.

[17] J. Lygeros, G. Pappas, and S. Sastry. An introduction to hybrid systems modeling, analysis and control. In *Preprints of the First Nonlinear Control Network Pedagogical School*, pages 307–329, 1999.

[18] M. A. Islam and A. Murthy. Supplementary document. `www.cs.sunysb.edu/~amurthy/hscc15_supp.htm`, 2014.

[19] M. A. Islam, A. Murthy, A. Girard, S. A. Smolka, and R. Grosu. Compositionality results for cardiac cell dynamics. In *Proceedings of the 17th International Conference on Hybrid Systems: Computation and Control*. ACM, 2014.

[20] MATLAB Open curve fitting toolbox (cftool). *Version 7.10.0 (R2010a)*. The MathWorks Inc., Natick, Massachusetts, 2010.

[21] R. Milner. *Communication and Concurrency*. Prentice Hall, 1989.

[22] S. Prajna and A. Jadbabaie. Safety verification of hybrid systems using barrier certificates. In *In Hybrid Systems: Computation and Control*, pages 477–492. Springer, 2004.

[23] S. Prajna, A. Jadbabaie, and G. J. Pappas. A framework for worst-case and stochastic safety verification using barrier certificates. *IEEE Transactions on Automatic Control*, 52(8):1415–1429, 2007.

[24] S. Prajna, A. Papachristodoulou, P. Seiler, and P. A. Parrilo. *SOSTOOLS: Sum of squares optimization toolbox for MATLAB*, 2004.

[25] S. Sankaranarayanan, X. Chen, and E. Abraham. Lyapunov function synthesis using Handelman representations. In *IFAC conference on Nonlinear Control Systems (NOLCOS)*, pages 576–581, 2013.

[26] M. A. B. Sassi, S. Sankaranarayanan, X. Chen, and E. Abraham. Linear relaxations of polynomial positivity for polynomial Lyapunov function synthesis, 2014.

[27] E. D. Sontag. Smooth stabilization implies coprime factorization. *IEEE Transactions on Automatic Control*, 34(4), 1989.

[28] E. D. Sontag. On the input-to-state stability property. *Systems and Control Letters*, 24:351–359, 1995.

[29] E. D. Sontag. Input to state stability: Basic concepts and results. In *Nonlinear and Optimal Control Theory*, pages 163–220. Springer, 2006.

[30] V. Iyer, R. Mazhari, and R. L. Winslow. A computational model of the human left-ventricular epicardial myocytes. *Biophysical Journal*, 87(3):1507–1525, 2004.

[31] V. A. Yakubovich, G. A. Leonov, and A. K. Gelig. Stationary sets in control systems with discontinuous nonlinearities (series on stability, vibration and control of systems, series a, vol. 14), 2004.

[32] Z. P. Jiang, I. M. Y. Mareels, and Y. Wang. A Lyapunov formulation of the nonlinear small-gain theorem for interconnected ISS systems. *Automatica*, 32(8):1211 – 1215, 1996.